FIELD MEASUREMENTS BASED MODEL FOR SURFACE IRRIGATION EFFICIENCY ASSESSMENT

D. Canone[1], M. Previati[1], I. Bevilacqua[1], L. Salvai[1], S. Ferraris[1,2]*

[1] Interuniversity Department of Regional and Urban Studies and Planning (DIST), Politecnico di Torino and Università di Torino, Castello del Valentino, viale Mattioli, 39, 10125 Torino, Italy

[2] ISAC-CNR, Istituto di Scienze dell'Atmosfera e del Clima, Corso Fiume 4, 10133 Torino, Italy

*Corresponding author: davide.canone@unito.it, Ph: +390110907428, +393405995796

Abstract

Within scenarios of water scarcity, the irrigation efficiency plays an increasingly strategic role. In this paper, a method that uses an advance-infiltration model based on four field measurements and the soil particle size distribution is proposed to estimate border-irrigation efficiencies. This method was applied to fifteen irrigation events and the application, storage and distribution efficiencies were estimated. The advance-infiltration model was validated against soil moisture measurements. The field-scale saturated hydraulic conductivity was estimated by model fitting to the measured depth of water infiltration. The sensitivity of the modelled irrigation efficiency to the operational surface irrigation parameters was evaluated by simulating seven irrigation scenarios based on field-collected data.

The infiltration profiles obtained by the proposed method were in agreement with the soil moisture measurements. The maximum difference between simulated and measured infiltration depth was 0.018 m . The field-scale saturated hydraulic conductivity values were in agreement with the infiltrometer tests results. The analysis of both simulated scenarios and monitored irrigation events highlighted the need for farmers to reduce the flow rates and increase the duration of irrigation events, in order to improve the irrigation efficiencies.

Keywords: agricultural hydrology; surface irrigation; irrigation efficiency; irrigation modelling.

1 Introduction

Because of the ever-increasing demand for water, analyses of irrigation efficiency have assumed an important role in Italy and throughout the entire Mediterranean area (Chohin-Kuper et al., 2003; Fereres and Soriano, 2007; Inglesias et al., 2007). Additionally, climate change is expected to increase water scarcity (Arnell, 1999; Inglesias et al., 2007).

On the western Po River Plain (Piedmont, northern Italy), where corn (*Zea mays* L.) is the most widely grown crop, surface irrigation systems are primarily used. Thus, for water resource management programmes (for which it is necessary to evaluate and reach a compromise between the constraints imposed by water scarcity and the production requirements) the analysis of the irrigation efficiencies of surface irrigation systems has become an essential tool.

To calculate the dependence of irrigation efficiency on irrigation parameters, three different strategies may be adopted: i) a detailed simulation of infiltration (e.g., Manzini and Ferraris, 2004; Ferraris et al., 2012); ii) a detailed simulation of infiltration coupled with the surface advance of water (e.g., Gandolfi and Savi, 2000); and iii) an analytical solution to the Lewis and Milne (1938) integral equation (Philip and Farrell, 1964).

Because the latter strategy requires a low number of parameters, it is suitable for providing a field-scale description of the rates of water advance and infiltration for practical uses (such as managing irrigation performance). In particular, when related to an infiltration function such as that of Philip (1957), which considers the saturated hydraulic conductivity, the Philip and Farrell analytical solution solves the advance-infiltration problem.

Although the Philip and Farrell analytical solution is only valid for short irrigation durations and cannot accurately predict long-term behaviour (Knight, 1980), this solution has been employed by several authors to successfully describe the advance-infiltration problem for surface irrigation management (e.g., Collis-George and Freebairn, 1979; Or and Silva, 1996).

The Philip (1957) infiltration function, used in the Philip and Farrell (1964) analytical solution, requires knowledge of soil hydraulic parameters to estimate the soil infiltration dynamics. Several authors have indicated that the Beerkan Estimation of Soil pedoTransfer (BEST) infiltration test proposed by Lassabatère et al. (2006) is an effective method for the hydraulic characterisation of soils directly in the field (e.g., Mubarak et al., 2009; Xu et al., 2009; Bagarello et al., 2011). Bagarello et al. (2011) investigated the possibility of simplifying the particle size distribution curve (PSD) fitting by including only three points (the clay, silt and sand contents) instead of fourteen points. These authors found the simplified PSD to be a reliable alternative to the normal procedure. Other methods have been recently developed for irrigation and management purposes (e.g.: Bautista et al., 2009; Strelkoff et al., 2009), which use surface water depth and mass balance methods to estimate the infiltration. Also, an interesting new analytical solution has been developed (Cook et al., 2013). However, it is beyond the scope of this paper to compare different analytical solutions. The proposed method is based on the direct measurement of the infiltration depth to calibrate the infiltration advance model, and to estimate the saturated hydraulic conductivity at the field scale. Within the context of ~~this~~ the above mentioned simplification, this study aims to propose a method for the calculation of border-irrigation efficiencies by using an advance-infiltration model and four simple field measurements: i) the inflow rate; ii) the irrigation duration; iii) the water head imposed on the field surface during an irrigation event and iv) the monitoring of the soil water content at only one point in the field at only the beginning and the end of the irrigation process. The second objective of this study was to use the proposed method to evaluate the surface irrigation efficiency of irrigation events based on the actual practices adopted by farmers. Hence, this method can provide a simulation tool that is able to analyse the effects of differences in management practices on irrigation efficiency.

2 Methodology

2.1 Advance-infiltration models

Irrigation efficiencies depend on the volume of water infiltrated during the irrigation event and on the distribution of the infiltrated water across the field. To compute the infiltrated volume of water and assess its distribution, it is necessary to determine the infiltration profile across the field. This infiltration profile can be obtained from the solution of the infiltration advance across the field. The infiltration advance is calculated from the simultaneous solution of two equations: the analytical solution to the Lewis-Milne (1938) differential equation proposed by Philip and Farrell (1964) to describe the advance of the water front and the infiltration equation of Philip (1957). These two equations are written as:

$$\frac{x}{q} = \frac{1}{C}\left[1 - exp\left(\frac{4C^2 t}{\pi \cdot S^2}\right) erfc \frac{2Ct^{1/2}}{\pi^{1/2} S}\right] \tag{1}$$

, and

$$I = S\sqrt{t} + Ct \tag{2}$$

,

where, x (L) is the horizontal spatial coordinate of the water advance front; q (L^2 T^{-1}) is the inflow rate per unit of width; C (L T^{-1}) is a parameter related to the saturated hydraulic conductivity K_S (L T^{-1}) according to the relation proposed by Haverkamp et al. (1988):

$$\frac{1}{3} K_S \leq C \leq \frac{2}{3} K_S \tag{3}$$

,

which depends on the initial soil water content; t (T) is the time; S (L $T^{-1/2}$) is the sorptivity; I (L) is the cumulative infiltration at any chosen value of x.

In this study, the parameter C was considered as constant and equal to $K_S/2$, as suggested by Parlange (1977). Such an assumption is valid because C is only slightly dependent on the initial water content (Philip 1957), and for most practical purposes, any change in C may be neglected. This assumption is not made because C does not change, but the changes in C are relevant for long-term infiltration rates, which are not considered in this work, and may be caused by changes in the saturated hydraulic conductivity (Samani and Yitayew 1989; Silva 1995) in association with changes in the near-surface soil porosity. Because long-term infiltration rates are not considered in this work, the Philip and Farrel analytical solution can be applied. In fact, the Philip and Farrell analytical solution should only be considered valid for short irrigation durations and should not be applied to accurately predict long-term behaviour (Knight, 1980). The method proposed by Knight

(1980) to verify short-duration conditions has been adopted in this work and is presented in the following section.

Sorptivity is defined as a function of the scale parameters of the water retention and hydraulic conductivity curves according to the relationship proposed by Parlange (1975):

$$S^2 = \int_{\theta_i}^{\theta_S} (\theta_S + \theta - 2\theta_i) K \frac{dh}{d\theta} d\theta \quad (4)$$

where, θ_S (L^3 L^{-3}) is the soil water content at saturation; θ (L^3 L^{-3}) is the actual soil water content; θ_i (L^3 L^{-3}) is the initial soil water content; K (L T^{-1}) is the soil hydraulic conductivity at θ; h (-L) is the actual matric potential.

In this study, the van Genuchten (1980) equation and the Brooks and Corey (1964) relationship were chosen as the models for calculating the water retention and hydraulic conductivity, respectively. The effect of hysteresis on the water retention curve was neglected, but it can be incorporated by including a hysteresis model, as suggested by Canone et al., 2008.

Hence, by integrating Eq. (4) within the water content range, one obtains:

$$S^2 = (\theta_i, \theta_S) = -C_p \theta_S K_S h_g \left(1 - \frac{\theta_i}{\theta_S}\right)\left[1 - \left(\frac{\theta_i}{\theta_S}\right)^{\eta}\right], \quad (5)$$

Where, h_g (-L) is the matric potential scale parameter of the van Genuchten (1980) equation; K_S (L T^{-1}) and η (L) are the scale parameter and shape parameter of the Brooks and Corey (1964) equation; C_p (-) is a soil-dependent constant (Haverkamp et al., 2006) depending on the shape parameters m and n of the van Genuchten (1980) equation.

Equation (1) is a function of S, K_S and q, and equation (2) is function of S and K_S. Since the method was applied to estimate the irrigation efficiency of border irrigation, the flow rate was measured at the inlet of a bay located at the centre of the field. The flow rate (q) was assessed by measurement of the cross-sectional area and the measurement of the current velocity. The latter was determined with a propeller flow meter OTT C2 (OTT Hydromet, Kempten, Germany, UE), which was installed before any irrigation monitoring and removed at the end of it. S and K_S are not directly measurable. In the proposed approach, the sorptivity is computed by solving equation (5), which requires the values of θ_S, θ_i, K_S, h_g, η, m and n.

The soil water content at saturation and the initial soil water content were measured at a time domain reflectometry (TDR) station located at one point in the field. The matric potential scale parameter (h_g) was calculated using the soil-independent conceptual model proposed by Vanclooster et al. (2011) to predict the soil water retention curve from the cumulative particle size distribution (PSD) curve and the void ratio.

In this study, the shape parameters m, n and η were determined from the PSD curve as suggested by Haverkamp et al., 2002. The PSD curve was fitted to five points obtained from the analysis of soil samples collected at an upstream, a centre and a downstream position along the bay under study. The particle size analysis was performed according to the pipette method, which is based on the difference in sedimentation speed between small and large soil particles. As demonstrated by Bagarello et al. (2011), the use of five points to fit a cumulative particle size distribution curve is sufficient for determining soil hydraulic parameters.

In the proposed approach, the saturated hydraulic conductivity ~~is~~ was the only parameter that cannot be measured. The field-equivalent value (K_{Seq}) ~~is~~ was determined by model fitting. Equations (1) and (2) were fitted to the depth of water infiltration at the end of an irrigation event. In Eqs. (1) and (2) C was considered equal to $0.5K_{Seq}$ and S was replaced by Eq. (5), so that only K_{Seq} was obtained by model fitting. The depth of water infiltration ~~is~~ was calculated from the water content data measured at the TDR station at the start and at the end of the irrigation event, following the methodology presented in section 2.5. The advance-infiltration model was validated against four depths of water infiltration at four times in-between the start and the end of the irrigation event.

The differences between the simulated (I_s) and measured (I_m) infiltration depth were compared to Cook et al. (2013) results employing the square root of the Nash-Sutcliffe efficiency coefficient (Nash and Sutcliffe, 1970), given by the following relation:

$$RSR = \frac{\sqrt{\sum_{i=1}^{N}\left(I_m(t_i)-I_s(t_i)\right)^2}}{\sqrt{\sum_{i=1}^{N}(I_m(t_i)-\bar{I}_m)^2}}, \quad (6)$$

where N is the number of simulated and measured infiltration depths and t is time (s).

Following the procedure explained above, the field equivalent sorptivity and the saturated hydraulic conductivity were determined once per year at each surveyed farm. These estimated field-equivalent parameters were used to calculate the advance-infiltration profiles for each irrigation event performed by the farmers and monitored within the study period.

Each saturated hydraulic conductivity value estimated using the proposed approach was compared to three values of saturated hydraulic conductivity estimated by BEST tests performed at the same location where the soil samples were collected, as explained in section 2.3. For the sake of comparison, the K_S values were also determined by seven pedotransfer functions based on particle size distribution data and θs (namely, Brakensiek et al., 1984; Cosby et al., 1984; Puckett et al., 1985; Saxton et al., 1986; Campbell and Shiozawa, 1994; Dane and Puckett, 1994; Ferrer-Julià et al., 2004).

2.2 Verification of the assumption of short irrigation duration

According to the limitations of the advance-infiltration model proposed by Philip and Farrell (1964) for predicting long-term infiltration processes, the short irrigation duration assumption has to be verified to employ this advance-infiltration model. In the proposed approach, the verification of the assumption is performed according to the methodology proposed by Knight (1980), which requires three variables. The first is a dimensionless time variable defined as:

$$\tau_k = K_S^2 t / S^2 \, . \quad (7)$$

The second is a dimensionless variable for the head on the soil surface given by:

$$C_k = K_S h_{surf} / S^2 \, , \quad (8)$$

where, h_{surf} (L) is the water head imposed on the field surface during the irrigation process.

The third is a dimensionless advancement variable given by the "linear" soil function proposed by Philip (1966, 1969), which, at small times, is given by the following equation when C ≠ 0:

$$x_k = \frac{\tau}{C_k} - \frac{2\tau^{3/2}}{3C_k^2} - \frac{\left(2C_k - \pi\right)\tau^2}{8C_k} - \frac{\left(2C_k^2 - 4C_k\pi + \pi^2\right)\tau^{5/2}}{15\pi C_k^4}. \qquad (9)$$

The dimensionless advancement is calculated by employing the linear soil function (Eq. 9) proposed by Philip (1966, 1969). Both the dimensionless advancement and time variables are compared to their maximum values (τ_{max} = 1.4 and x_{max} = 0.4), which are the limits of the area of a τ-x_k plot for which the time can be considered short. Because the Philip and Farrell advance-infiltration model behaves as the linear soil function, proposed by Philip (1966, 1969), for any values of C_k within the range between 0 and 2 (Knight, 1980), the short duration assumption is verified for τ_k and x_k values lower than τ_{max} and x_{max}, respectively.

2.3 Saturated hydraulic conductivity validation

In this study, the BEST infiltration test (Lassabatère et al., 2006) was employed to obtain an estimation of K_S that is independent from the advance-infiltration model and the soil water content measured by the TDR station. These independent values of K_S were determined once a year at the same locations where the soil samples were collected. They were compared to the K_{Seq} values estimated following the methodology presented in section 2.1 to validate the latter.

In the BEST procedure, the scale parameter for the residual water content (θ_r) was assumed to be zero, and the initial soil water content and the soil water content at field saturation (θ_S) were estimated using the TDR measurements collected before and after the infiltration tests. The values of K_S and S were determined by fitting the experimental infiltration data to the set of equations proposed by Lassabatère et al. (2006). Finally, the scale parameter for the matric potential (h_g) for the water retention curve of van Genuchten (1980) was obtained using Eq. (5).

2.4 Farm descriptions

Three farms, characterized by their analogous soil conditions were selected as testing sites. All farms performed border irrigation on corn (*Zea mays* L.) crops. These farms are located in the

Cuneo district (namely: farm 1, Ceresole d'Alba, Lat. 44° 48' 37", Lon. 7° 46' 45"; farm 2, Fossano, Lat. 44° 34' 40", Lon. 7° 42' 06"; farm 3, Sommariva del Bosco, Lat. 44° 44' 21", Lon. 7° 43' 33") in north-western Italy. The soil of the three farms, were analysed according to the USDA Keys to Soil Taxonomy (Soil Survey Staff, 2010), and belong to the following families: farm 1, Fluventic Dystrudept, coarse-loamy, mixed, nonacid, mesic; farm 2, Acquic Haplustept, coarse-loamy over loamy-skeletal, mixed, nonacid, mesic; farm 3, Acquic Haplustept, loamy-skeletal,mixed,nonacid,mesic.

Despite the fact that the soils belonged to similar textural classes (i.e., loam and silty loam), the soils exhibited differences in their hydraulic properties (e.g., the soil water content at saturation conditions and the field capacity, listed in Table 1) primarily because of the differences in tillage practices and the varying percentages of stones in the fields. The percentages of sand, clay, and silt (defined according to the USDA Classification System (Soil Survey Laboratory Staff, 1992)) are included in Table 2 and were calculated from the average of the laboratory analysis of four samples collected at four different depths (between 0.05 m and 0.6 m). The percentages of stones were determined from the analysis of two vertical soil profiles for each field. These analyses were performed during the 2007 irrigation season.

During the three-year period (2006-2008), the farmers executed thirty irrigation events, and fifteen were monitored with specific measurement campaigns. In such a period, the border sizes of these farms changed (Table 3) because the farmers autonomously followed their normal habits regarding cultivation management and irrigation practices. However, the practices of the farmers are crucial for the study because monitoring real-world agriculture was one of the study's main objectives. All farmers cultivated the corn (*Zea mays* L.) on bays composed by multiple rows (10 rows per bay at farm 1, 13 rows per bay at farm 2, and 8 rows per bay at farm 3) with interrow spacing of 0.75 m. The rows were oriented along the maximum field length. At the end of the field a small canal to collect surface runoff was seasonally dug.

2.5 TDR stations

Time Domain Reflectometry is a well-known technique that is commonly accepted for the assessment of water content and other physical properties of porous media by permittivity measurements (Topp et al., 1980; Robinson et al., 2003; Canone et al., 2009; Baudena et al., 2012; Previati et al., 2012). Soil permittivity measurements were carried out using a device composed by one TDR cable tester (Tektronix Metallic Cable Tester 1502C manufactured by Tektronix Inc., Beaverton, OR, USA) connected to a notebook and a multiplexer. The system allowed automatic measurements of soil permittivity at eight points along the soil profile. The TDR signals were sampled and acquired using the WinTDR software (Or et al., 2004) and stored in the hard disk of a notebook. The soil bulk permittivity was monitored from the beginning to the end of the irrigation events at a time interval of 3 minutes, and the volumetric soil water content was computed using the composite dielectric approach described by Roth et al. (1990).

The installed TDR probes were 150 mm long and were composed of three stainless steel rods held together by a nylon spacer. All of the probes were calibrated according to the method proposed by Heimovaara (1993). All of the connections were made using RG58 50 Ω coaxial cables. Each of the 10 probes was horizontally inserted into the soil. The probes were arranged in two vertical profiles at the depths of 0.05 m, 0.15 m, 0.30 m, 0.45 m, and 0.65 m to monitor the entire root zone. In one of the fifteen examined cases, a layer of stones prevented the 0.65 m depth measurement (Fig. 1). The TDR stations were located at approximately one-third of the field length along a bay situated at the centre of the field.

Each volumetric water content measurement was then associated with and weighted in relation to its specific corresponding volume of soil (equivalent to the thickness of each monitored layer). In other words, the value obtained by the probe placed at a depth of 0.05 m was considered representative of the soil layer between 0 m and 0.10 m depth, whilst the soil water content value obtained by the 0.15 m depth probe was considered representative of the soil layer between 0.10 m and 0.225 m of depth, and thus forth for the deeper probes. Thus, the volumes of water that infiltrated the soil and the evolution of the water content profiles over time during the irrigation process (Fig. 2) were obtained for the three farms.

2.6 The measurements of irrigation parameters

Field measurements were performed to acquire the following data for each monitored irrigation event: i) the duration of the irrigation event, t_{ir} (T); ii) the irrigation inflow rate, F_r ($L^3\ T^{-1}$); iii) the volume of water delivered during the irrigation event, V_d (L^3), and average volume of water delivered per unit area, ($L^3\ L^{-2}$); and iv) the water head imposed on the field surface during the irrigation event, h_{surf} (L), which was measured by a water level staff gauge (marked at every millimetre) under steady flow conditions at the upstream position. We also recorded the occurrence of surface runoff, the time at which the surface runoff was eventually starting. The volume of surface runoff and deep percolation were not measured. They were calculated from the partition of the applied water volume determined from infiltration profiles as explained in the following section. Furthermore, the number of irrigation events initiated during the season by each farmer, the irrigation parameters and the infiltration advance profiles were used to partition the applied water volumes.

2.7 Partitioning of the applied water volume

The volume of storable water at field capacity V_{fc} (L^3) was calculated by multiplying the water content at field capacity by the volume of soil in the root layer. The soil water content at field capacity was calculated as the soil water content value given by the van Genuchten (1980) equation for the matric potential value of -3.3 m. Using the infiltration advance profiles and the scheme given in Figure 3, the volume of water applied to the field was partitioned as follows: i) the total volume of water stored in the soil V_{st} (L^3), which was calculated by subtracting the water volume lost through deep percolation from the total infiltrated volume and then adding the volume stored on the surface; ii) the volume stored at the surface V_s (L^3), which is the volume of water on the surface of the field after the completion of the water application; iii) the volume of water lost by surface runoff

V_r (L^3), which was calculated as the sum of the infiltrated water volume and the volume of water stored on the land surface beyond the end of the field (when the irrigation ended); and iv) the volume lost through deep percolation below the root layer V_{dp} (L^3). The volume of water stored on the surface (V_s) was divided into two parts. The amount of the V_s that remained on the portion of the field where deep percolation occurred was considered lost. The remaining volume was added to the stored volume. The errors introduced by such assumptions are small because V_s never exceeded 10% of the stored volume (Table 4).

The volumes of water lost by surface runoff and deep percolation were not measured. They were calculated from the infiltration profiles given by the infiltration advance model. Considering that the model was validated on the infiltrated water depth at the locations of the TDR stations (as shown in section 3.1) and the aim of the work was to employ simple measurement techniques, we choose not to measure the volume of water lost by runoff and deep percolation. Such measurements were not necessary for the validation of the model and their acquisition would have severely complicated the field measurement campaigns.

All calculated water volumes were used to compute the application efficiency (E_a), the storage efficiency (E_s), and the distribution efficiency (E_d) terms for the field-equivalent parameters. For further comparison, the efficiency terms were also calculated for the three sets of parameters determined by the infiltration BEST tests. Finally, the proposed model was used to simulate the effects of changes in various irrigation parameters, namely, the flow rate (F_r), the irrigation event duration (t_{ir}), the volume of water delivered (V_d) and the initial soil moisture θ_i.

2.8 Irrigation efficiencies

The application efficiency (E_a) quantifies the volume of water actually stored in the root layer in relation to the volume of water delivered. The storage efficiency (E_s) quantifies the recovery of the field water deficit. The distribution efficiency (E_d) quantifies the homogeneity of water storage along the field. The combination of these three efficiency terms provides the global efficiency of the irrigation process. Additionally, by employing the proposed method, the choice of the best irrigation practice may be achieved.

The water application and storage efficiencies are given according to the relationships proposed by Kruse et al. (1990):

$$E_a = \frac{V_{st}}{V_d}, \tag{10}$$

$$E_s = \frac{V_{st}}{V_{fc}}, \tag{11}$$

The distribution efficiency is determined using the relationship proposed by Burt et al. (1997):

$$E_d = \frac{V_{lq}}{V_{fq}}, \tag{12}$$

where, V_{lq} is the volume of water stored in the last quarter of the field (L^3), whilst V_{fq} is the volume stored in the first quarter of the field (L^3).

2.9 Predictive simulations

After the irrigation efficiencies of the monitored events were calculated, and the model was employed to predict the irrigation efficiencies of simulated irrigation events. In particular, the irrigation simulations were performed using seven different combinations of the irrigation parameters (i.e., V_d, F_r and θ_i) to determine their influence on irrigation efficiency. The values of the irrigation parameters are presented and discussed in section 3.4.

3 Results and Discussion

3.1 Model validation

The first step of the model validation was the confirmation of the short duration assumption. For the measured irrigation times used in this study, the calculated values of x_k and τ_k, as proposed by Knight (1980), corresponded to a short-duration behaviour. These parameter values are given in Table 5. The dimensionless time and advancement variables never exceeded the maximum values (τ_{max} = 1.4 and x_{max} = 0.4) proposed by Knight (1980). According to Knight (1980), employing this combination of values ensures that the behaviour of the Philip and Farrell analytical solution matches the actual advance-infiltration processes.

Using the proposed method, the field-equivalent saturated conductivity (K_{Seq}) values, obtained by fitting of Eqs. (1,2 and 5) as explained in section 2.1, were close to the three sets of values estimated by the BEST infiltration tests (Tables 6 and 7). The differences among the K_{Seq} values and the results of the corresponding BEST tests were almost always lower than 16% of the K_S values obtained from BEST tests. Only two differences exceeded that range. Both values were recorded at Farm 2, one in the year 2007 (36.7%) and the other in the year 2008 (-40.9%), as shown in Table 7. The results of the BEST tests indicated low K_S variability across the fields of Farm 1 and Farm 3, as shown by the standard deviation of K_S values (Table 6) and by the three K_S values measured at each field, and among the three-year period (Table 7). The low variability of K_S was probably attributed to the tillage practices: each year, the soil structure was effectively destroyed by the rototilling practices performed prior to sowing. In any case, for further comparison, the root mean square error (RMSE) between the results of seven different pedotransfer functions applied for the estimation of K_S and the K_{Seq} values were evaluated. The RMSE between the results of the BEST tests and the K_{Seq} values were also evaluated. The K_S values are depicted in Figure 4 and the RMSE are listed in Table 8. Only one of the seven pedotransfer functions (Puckett et al., 1985) produced results that are in agreement with the estimated K_{Seq} values.

The infiltration depths of water were then compared with the infiltration profiles, which were calculated using the fitted K_{Seq} values (Table 6), the K_S values obtained by the BEST tests, and the irrigation parameters chosen by the farmers. The infiltration depths were obtained from the TDR soil water content measurements. Finally, the differences between the infiltration profiles and the infiltrated depth of water were assessed. The infiltration model outputs were always in good agreement with the measured infiltration depths (Fig. 5), as shown by the differences between simulated and measured infiltration depths reported in Table 9. The highest and the lowest differences recorded during the fifteen monitored events were 0.018 m and 0.002 m. The SRS calculated to evaluate the performance of the proposed method on the monitored irrigation events was 0.22 at Farm 1, 0.07 at Farm 2 and 0.05 at Farm 3. Cook et al. (2013) found SRS values between 0.29 and 6.83 for the Philip and Farrel (1964) infiltration-advance solution for short-term duration. The low SRS obtained in our experiments is due to the direct measurement of the infiltration depth. Cook et al. (2013) employed infiltration depths estimated by Taylor (1981) using the mass balance method of Finkel and Nir (1960). The highest difference between the simulated and measured data observed during the first irrigation event performed by farm 1 in 2007 was 0.013 m. This difference was recorded at a station located 30 m from the beginning of the field at 720 s and 913 s (t_{ir}) after the start of irrigation. The simulated infiltration depths were 0.178 m and 0.203 m, respectively, and the measured depths were 0.191 m and 0.216 m, respectively. The minimum difference occurred during the same irrigation event, was recorded at 360 s after the start of irrigation, at a station located 32 m from the beginning of the field. The simulated infiltration depth was 0.116 m and the measured depth was 0.114.

3.2 Irrigation efficiencies vs. hydraulic parameters

As expected from Eqs. 1, 2 and 5, the analysis of the influence of the initial water content on the volume of water that might infiltrate the soil demonstrates the relationship between θ_i and the irrigation efficiency. The analysis of irrigation events performed at the constant values of K_S and F_l, and similar values of F_r, indicate that a high θ_i results in low E_a values because of the low infiltration rate and, consequently, high surface runoff. Moreover, high θ_i values indicate a low soil retention capacity, which results in deep percolation losses even during low infiltration events.

The K_{Seq} values and the three K_S values estimated by the BEST infiltration tests were used to calculate four sets of efficiency values. The analysis of the application and storage efficiency values indicates that K_S has only a minor influence on the results (Figs. 6a and 6b) because the variability in K_S was very low. The low variability in K_S values could only transform deep percolation losses into runoff losses when there was little change in the volume of water stored in the root layer. Thus, the distribution efficiency is more highly influenced by K_S than the other two efficiencies (Fig. 6c) because it depends on the shape of the infiltration profile and can be modified by small variations in K_S. The variation among the E_a values of the irrigation events was negligible (below 0.05) in almost all cases. As indicated in Figure 6a, we observed the highest variation of E_a in the first irrigation performed on farm 3 in 2006 (0.06). The variation among the E_s values was also negligible in almost all cases; the highest value was also observed for the first irrigation performed on farm 3 in 2006 (0.07), as shown in Figure 6b. The variation among E_d values was negligible for six of the fifteen irrigation events monitored; the highest E_d value was again observed for the first irrigation performed on farm 3 in 2006, as shown in Figure 6c, but this value was much higher (0.27) than the values found for E_a and E_s.

3.3 Irrigation efficiencies vs. irrigation parameters

The irrigation parameters varied considerably during the study period. In fact, the farmers were completely free to manage the irrigation events. Relying on their experience and on an empirical evaluation of the soil water content, many farmers tried to limit the effect of the initial water content by varying the volume of irrigation water and, in several cases, the flow rate (Table 10). Because of farm management needs, the farmers also changed the lengths of several plots during the three-year period.

The variations in the lengths of the plots, combined with a non-proportional variation in the flow rate and the temporal variability of the field-scale saturated hydraulic conductivity, resulted in variations in the time required for the water to reach the end of the field (t_{fl}). Additionally, this variation caused i) a modification of the time required to impose a uniform hydraulic head over the entire field surface and ii) a change in the volume of infiltrated water that, in some cases, was large enough to mask the effects of the initial water content. To limit the effects of the farmers' choices and to assess the real influence of t_{fl} and θ_i on irrigation efficiency, the analysis was conducted on pairs of irrigation events in which the other parameters were maintained nearly as constants.

As indicated in Eqs. (1) and (5), the analysis of irrigation events performed with constant values of K_S and F_l and similar values of F_r indicate that the effect of t_{fl} on irrigation efficiency is inversely proportional to θ_i. High θ_i values are associated with low t_{fl} values, which result in low E_a values because of the high surface runoff. Low t_{fl} values are associated with the rapid imposition of a constant head over the bay, which causes high values of E_s and E_d (Figs. 6b, 6c). Only a few exceptions were found. In the examined pairs of irrigation events, the exceptions were explained by the differences in t_{ir} and F_r employed by the farmers.

By employing higher flow rates, each of the farms achieved higher distribution efficiency values. However, because of the surface runoff, the benefits of a higher E_d often did not compensate for the decrease in the application efficiency values. The irrigation time (t_{ir}) cannot be decrease to approach t_{fl} to avoid surface runoff because a low t_{ir} would cause a great difference in the time of infiltration between upstream and downstream areas, which would strongly reduce the distribution efficiency values. The best compromise was often achieved by modifying the flow rate. However, if the irrigation district is provided with a network of gully channels, the volumes of water lost as surface runoff should not be counted among the losses that affect the application efficiency (Clemmens et al., 2008).

In most cases, the volumes of water stored during the monitored irrigation events balanced the hydraulic deficit of the root layer. However, whilst the irrigations performed at farm 1 resulted in water storage efficiencies that were significantly lower than one, all of the irrigations performed at farm 2 and 3 resulted in higher E_s values, but with the disadvantage of high deep-percolation losses.

3.4 Scenario analysis and considerations for predictive settings

The infiltration profile across the entire field, which was simulated using the actual parameters of the first irrigation event that was performed at farm 1 in 2007 (Fig. 7a), was compared with the infiltration profiles produced by seven irrigation simulations. In the first three cases (Figs. 7b to 7d), the duration of the irrigation event and the flow rates were altered. The infiltration profiles described by cases 4-7 (Fig. 7e to 7h) were produced with differing flow rates and initial water contents. The values of the input parameters employed in the simulations are summarized in Table 11 in addition to the simulation results.

In the first case (Fig. 7b), the flow rate was reduced to a value of 0.04 (m^3 s^{-1}), whilst the duration of the irrigation event was increased by approximately one-third (1200 s) (Table 11). In this case, an E_a value of 0.95 was achieved because the water flowed only slightly past the end of the field and slightly deeper than the bottom of the soil root layer; hence, there were only small amounts of surface runoff and percolation losses. Although the watering volume of this first case was greater than that of the real monitored case, the majority of the water was stored equally and the E_s was slightly improved because of this level of storage. In contrast, there was a reduction in E_d that caused a reduction in the overall irrigation efficiency.

In the second case (Fig. 7c), the flow rate was equal to the previous case (Table 11), but the duration of the irrigation event was increased by one-third (1600 s). The results indicate an improvement in the E_s and E_d and a decrease in the E_a value. The watering volume considered in this case was higher than the two previous cases, which suggests that the necessary watering volume was surely underestimated for the monitored case.

In the third case (Fig. 7d), the flow rate was the same as in the real irrigation event, whilst the event duration was the same as in the second case, thus applying a watering volume that was almost twice as large as the volume of the real irrigation event. In this case, both the E_s and E_d increased to a value of 1, but the E_a value (0.64) was the lowest among all of the cases considered (Table 11).

In the fourth case (Fig. 7e), the flow rate was increased to a value of 0.06 (m^3 s^{-1}) but the irrigation duration was maintained at the actual value used by the farmer (Table 11). Compared to the real irrigation event, the results indicate an increase in the E_s (+0.04) and E_d (+0.10) and a decrease in the E_a (-0.11). The E_a value was comparable to the value obtained in the second case, but the E_s and E_d values were lower.

In the fifth case (Fig. 7f), the flow rate was increased to a value of 0.07 (m^3 s^{-1}), whilst the irrigation event duration was maintained at the actual irrigation duration. Compared to the previous case, the E_s and E_d increased slightly (+0.02 and +0.07, respectively). In this case, the E_a value was slightly lower than in the second case, whilst the storage efficiency value decreased by 0.12.

In the sixth case (Fig. 7 g), the flow rate and the irrigation event duration values were the same as the values from the real irrigation event (Table 11), but the initial soil water content was set to a value of 0.05 ($m^3 m^{-3}$), which is lower than the measured value. Compared to the real event, the results suggest an increase in the E_a (+0.05) because of the higher infiltration rate caused by the high value of the matric potential, which is inversely proportional to the soil water content.

When compared to the real irrigation event, the results of the first six cases also indicate a reduction in the E_s because the water deficit was higher in these simulations. Additionally, the results demonstrate a reduction in the E_d because of the difference in the depth of water infiltration at the beginning and at the end of the field during the time required to establish a uniform hydraulic head over the field. The simulation results suggest that, when the irrigation is performed at a θ_i that is lower than in the actual irrigation event considered, the flow rate should be increased.

Finally, in the seventh simulation (Fig. 7 h), the initial water content was assumed to be higher than the real value and was set to a value of 0.15 ($m^3 m^{-3}$). However, the other parameters were the same as in the real irrigation event (Table 11). As expected, the results were the opposite of the previous case. Compared to the real event, the E_a decreased (-0.06) and both the E_s and E_d increased to +0.12 and +0.10, respectively.

According to the simulation results, the best E_a value was obtained for the sixth case, but the corresponding E_s and E_d values were the lowest. This result suggests that this choice would represent a misuse of water. In contrast, the best E_s and E_d values were registered in the third case, but the E_a value was the lowest. The real irrigation event considered represents a compromise between saving water and the best use of water for crop production. The second case is also a good compromise because a slightly greater volume of water is employed to obtain a large increase in E_s

and E_d. A higher flow rate was not always the best solution. A comparison between the results of the fourth and fifth cases indicates that a high flow rate could be employed to increase the E_s and E_d values. However, this solution can only be applied in cases where the irrigation district is provided with a network of gully channels to avoid surface runoff losses and maintain high values of E_a.

For the monitored irrigation events, the flow rate employed by the farmer was suitable for the field conditions, whereas the watering volume was insufficient, as shown in the third simulation (Fig. 7d). Similar to the previous simulations, the sixth and seventh simulations (Fig. 7 g and 7 h) demonstrated the influence of the initial field conditions. These results suggest that farmers should apply larger watering volumes, but less frequently, to obtain higher irrigation efficiencies. Moreover, to avoid low E_s and E_d values, irrigation should not be performed when the soil water content is too low.

5 Conclusions

In this study, a method based on the Philip and Farrel (1964) advance-infiltration model was proposed for i) calculating the border irrigation efficiency from four simple field measurements (inflow rates, irrigation durations, and soil water content values monitored at only one point of the field at the beginning and at the end of the irrigation processes) and ii) for testing the sensitivity of irrigation efficiency to surface irrigation operational parameters.

The irrigation efficiency of 15 real irrigation events performed on three different farms during the growing seasons in 2006, 2007 and 2008 were analysed. Finally, a scenario analysis based on data collected during one of the surveyed events was also performed by altering the irrigation parameters that affect irrigation efficiency (namely, irrigation duration, flow rate, and initial soil water content). The proposed method proved to be capable of describing real irrigation practices. Moreover, the method was capable of evaluating the changes in irrigation efficiency as a consequence of variations in the operational irrigation parameters.

The results demonstrate that the equivalent saturated hydraulic conductivities estimated using the proposed method is always in good agreement with the K_S values estimated using the infiltration tests performed at three different positions in each field. Additionally, the irrigation efficiencies calculated using both the proposed approach and using the parameters estimated by infiltration measurements were in good agreement.

The efficiencies analysis (of the water application, storage, and distribution efficiencies) highlighted the marked variability in the values among the monitored farms and within each farm. This level of variability was associated with the variations in the watering volumes and flow rates. The influence of the initial soil water content on the storage efficiency was clear, but some exceptions were observed when irrigation durations was sufficiently long to mask the effects of the initial soil water content.

The analysis of both the simulated scenarios and fifteen monitored irrigation events demonstrated the need to irrigate these fields using lower flow rates and higher irrigation durations than those currently used by the farmers. The scenario analysis also revealed that the irrigation efficiencies are highly dependent on the initial soil water content.

6 Acknowledgements

This study was partially funded by the Italian Ministry of Research through Italian Research Project of Relevant Interest (PRIN2010-2011), prot. 20104ALME4, “National network for monitoring, modeling, and sustainable management of erosion processes in agricultural land and hilly-mountainous area” (PI Mario Aristide Lenzi) and through the project PRIN2010-11 “New methodologies for water resources management in hydro-climatic uncertainty scenarios” (PI Alberto Bellin).

Special thanks are given to all of the staff of the Coldiretti Cuneo, to the farmers for their endless patience and to Prof. Randel Haverkamp for his helpful suggestions.

7 References

Arnell, N.W., 1999. Climate change and global water resources. Global Environ. Change 9, S31-S49.

Bagarello, V., Di Prima, S., Iovino, M., Provenzano, G., Sgroi, A., 2011. Testing different approaches to characterize Burundian soils by the BEST procedure. Geoderma 162, 141-150.

Baudena, M., Bevilacqua, I., Canone, D. , Ferraris, S., Previati, M., Provenzale, A., 2012. Soil water dynamics at a midlatitude test site: Field measurements and box modeling approaches. J. Hydrol. 414-415, 329-340. doi: 10.1016/j.jhydrol.2011.11.009

Bautista, E., Clemmens, A.J., Strelkoff, T.S., 2009. Structured Application of the Two-Point Method for the Estimation of Infiltration Parameters in Surface Irrigation. J. Irrig. Drain. Eng. 135(5), 566–578.

Brakensiek, D.L., Rawls, W.J., Stephenson, G.R., 1984. Modifying SCS hydrologic soil groups and curve numbers for rangeland soils. ASAE Paper No. PNR-84-203, St. Joseph, MI.

Brooks, R.H., Corey, A.T., 1964. Hydraulic properties of porous media. Hydrology Paper 3, Colorado State University, Fort Collins, CO, USA.

Burt, C.M., Clemmens, A.J., Strelkoff, T.S., Solomon, K.H., Bliesner, R.D., Hardy, L.A., Howell, T.A., Eisenhauer, D.E., 1997. Irrigation Performance Measures: Efficiency and Uniformity. J. Irrig. Drain. E-ASCE 123(6), 423-442. doi:10.1061/(ASCE)0733-9437(1997)123:6(423)

Campbell, G.S., Shiozawa, S., 1994. Prediction of hydraulic properties of soils using particle-size distribution and bulk density data. In: van Genuchten, M.T., Leij, F.J., Lund, L.J. (Eds.), Proceedings of the International Workshop on Indirect Methods for Estimating the Hydraulic Properties of Unsaturated Soils, University of California, Riverside, CA, pp. 317-328.

Canone, D., Previati, M., Ferraris, S., Haverkamp, R., 2009. A New Coaxial Time Domain Reflectometry Probe for Water Content Measurement in Forest Floor Litter. Vadose Zone J. 8, 363-372.

Canone, D., Ferraris, S., Sander, G., Haverkamp, R., 2008. Interpretation of water retention field measurements in relation to hysteresis phenomena. Water Resour. Res. 44, W00D12. doi: 10.1029/2008WR007068

Chohin-Kuper, A., Rieu, T., Montginoul, M., 2003. Water Policy Reforms: Pricing Water, Cost Recovery, Water Demand and Impact on Agriculture. Lessons from the Mediterranean experience, at the water pricing seminar, June/July 2003, Agencia Catalana del Agua and World Bank Institute, Barcelona. http://www.emwis.net/documents/database/water-policy-reforms-pricing-water-cost-recovery. Last checked 25/09/2013.

Clemmens, A.J., Allen, R.G., Burt, C.M., 2008. Technical concepts related to conservation of irrigation and rain water in agricultural systems. Water Resour. Res. 44, W00E03. doi: 10.1029/2007WR006095

Collis-George, N., Freebairn, D.M., 1979. A laboratory and field study of border check irrigation. Aust. J. Soil Res. 17, 75-87.

Cook, F.J., Knight, J.H., Doble, R.C., Raine, S.R., 2013. An improved solution for the infiltration advance problem in irrigation hydraulics. Irrig. Sci. 31, 1113-1123.

Cosby, B.J., Hornberger, G.M., Clapp, R.B., Ginn, T.R., 1984. A statistical exploration of the relationship of soil moisture characteristics to the physical properties of soils. Water Resour. Res. 20 (6), 682-690.

Dane, J.H., Puckett, W., 1994. Field soil hydraulic properties based on physical and mineralogical information. In: van Genuchten, M.T., Leij, F.J., Lund, L.J. (Eds.), Proceedings of the International Workshop on Indirect Methods for Estimating the Hydraulic Properties of Unsaturated Soils, University of California, Riverside, CA, pp.389-403

Fereres, E., Soriano, M.A., 2007. Deficit irrigation for reducing agricultural water use. J. Exp. Bot. 58, 147–159.

Ferraris, S., Bevilacqua, I., Canone, D., Pognant, D., Previati, M., 2012. The finite volume formulation for 2-D second-order elliptic problems with discontinuous diffusion/dispersion coefficients. Math. Probl. Eng. 2012, 1-23. doi: 10.1155/2012/187634

Ferrer-Julià, M., Estrela Monreal, T., Sánchez del Corral Jiménez, A., García Meléndez, E., 2004. Constructing a saturated hydraulic conductivity map of Spain using pedotransfer functions and spatial prediction. Geoderma 123, 275-277.

Finkel, H.J., Nir, D., 1960. Determining infiltration rates in an irrigation border. J. Geophysical Res. 65(7), 2125-2131.

Gandolfi, C., Savi, F., 2000. A Mathematical Model for the Coupled Simulation of Surface Runoff and Infiltration. J. Agr. Eng. Res. 75, 49-55.

Haverkamp, R., Kutilek, M., Parlange, J.-Y., Rendon, L., Krejka, M., 1988. Infiltration under ponded condition: 2. Infiltration equation tested for parameter time dependence and predictive use. Soil Sci. 145, 317-329.

Haverkamp, R., Nimmo, J.R., Reggiani, P., 2002. Property-Transfer Models. In: Dane, J., Topp, G.C. (Eds.), Methods of Soil Analysis, Vol.4: Physical Methods. Soil Science Society of America, Madison, Wisconsin.

Haverkamp, R., Debionne, S., Viallet, P., Angulo-Jaramillo, R., Decondappa, D., 2006. Movement of moisture in the unsaturated zone. In: Delleur, J.W. (Ed.), Groundwater Engineering Handbook. 2nd ed., CRC Press LLC, Boca Raton, Florida.

Heimovaara, T.J., 1993. Design of triple wire Time Domain Reflectometry probes in practice and theory. Soil Sci. Soc. Am. J. 57,1410-1417.

Inglesias, A., Garrote, L., Flores, F., Moneo, M., 2007. Challenges to Manage the Risk of Water Scarcity and Climate Change in the Mediterranean. Water Resour. Manage. 21, 775–788.

Knight, J.H., 1980. An improved solution for the infiltration advance problem in irrigation hydraulics. 7^{th} Australasian hydraulics and fluids mechanics conference, Brisbane, 18-22 august 1980.

Kruse, E.G., Bucks, D.A., von Bernuth, R.D., 1990. Comparison of irrigation systems. In: Stewart, B.A. and Nielsen, R. (Eds.), Irrigation of agricultural crops. ASA-CSSA-SSSA. Madison, Wisconsin.

Lassabatère, L., Angulo-Jaramillo, R., Soria Ugalde, J.M., Cuenca, R., Braud, I., Haverkamp, R., 2006. Beerkan Estimation of Soil Transfer Parameters Trough Infiltration Experiments - BEST. Soil Sci. Soc. Am. J. 70, 521-532. doi:10.2136/sssaj2005.0026

Lewis, M.R., Milne, W.E., 1938. Analysis of border irrigation. Agric. Eng. 19, 267-272.

Manzini, G., Ferraris, S., 2004. Mass-conservative finite volume methods on 2-D unstructured grids for the Richards' equation. Adv. Water Resour. 27(12), 1199-1215. doi:10.1016/j.advwatres.2004.08.008

Mubarak, I., Mailhol, J.C., Angulo-Jaramillo, R., Ruelle, P., Boivin, P., Khaledian, M., 2009. Temporal variability in soil hydraulic properties under drip irrigation. Geoderma 150, 158–165.

Nash, J.E., Sutcliffe, J.V., 1970. River flow forecasting through conceptual models: part 1. A discussion of principles. J. Hydrol. 10(3), 282-290.

Or, D., Silva, H. R., 1996. Prediction of surface irrigation advance using soil intake properties. Irrig. Sci. 16, 159-167.

Parlange, J.-Y., 1975. On solving the flow equation in unsaturated soils by optimization: Horizontal infiltration. Soil Sci. Soc. Am. J. 39, 415–418.

Philip, J.R., 1957. The theory of infiltration: 1. The infiltration equation and its solution. Soil. Sci. 83, 345-357.

Philip, J.R., Farrell, D.A., 1964. General solution of the infiltration-advance problem in irrigation hydraulics. J. Geophys. Res. 69, 621–631.

Philip, J.R., 1966. A linearization technique for the study of infiltration. In: Rijtema, R.E., Wassink, H. (Eds.), Water in the Unsaturated Zone, Proc. UNESCO Symp. 1, 471-478.

Philip, J.R., 1969. Theory of infiltration. Adv. Hydrosci. 5, 215-296.

Previati, M., Canone, D., Bevilacqua, I., Boetto, G., Pognant, D, Ferraris, 2012. Evaluation of wood degradation for timber check dams using time domain reflectometry water content measurements. Ecol. Eng. 44, 259-268.

Puckett, W.E., Dane, J.H., Hajek, B.F., 1985. Physical and mineralogical data to determine soil hydraulic properties. Soil Sci. Soc. Am. J. 49, 831–836.

Robinson, D.A., Jones, S.B., Wraith, J.M., Or, D., Friedman, S.P., 2003. A review of advances in dielectric and electrical conductivity measurements in soils using Time Domain Reflectometry. Vadose Zone J. 2, 444–475.

Roth, K., Schulin, R., Flühler, H., Attinger, W., 1990. Calibration of Time Domain Reflectometry for water content measurement using a composite dielectric approach. Water Resour. Res. 26(10), 2267-2273.

Saxton, K.E., Rawls, W.J., Romberger, J.S., Papendick, R.I., 1986. Estimating generalized soil water characteristics from texture. Soil Sci. Soc. Am. J. 50, 1301-1036.

Soil Survey Laboratory Staff, 1992. Soil survey laboratory methods manual. Soil Survey Investigations Report n°42, Version 2.0. USDA-SCS U.S. Government Printing Office, Washington D.C.

Soil Survey Staff, 2010. Keys to Soil Taxonomy, 11th ed. USDA-Natural Resources Conservation Service, Washington, DC.

Strelkoff, T.S., Clemmens, A.J., Bautista, E., 2009. Estimation of soil and crop hydraulic properties. J. Irrig. Drain. Eng. 135(5), 537–555.

Taylor, A.R., 1981. A method for surface irrigation design based on infiltration using the border strip as an infiltrometer. PhD Thesis, University of Canterbury, Lincoln College, 229 pages.

Topp, G.C., Davis, J.L., Annan, A.P., 1980. Electromagnetic determination of soil water content: measurements in coaxial transmission lines. Water Resour. Res. 16 (3), 574–582.

van Genuchten, M.T., 1980. A closed form equation for predicting the hydraulic conductivity of unsaturated soils. Soil Sci. Soc. Am. J. 44, 892-898.

Xu, X., Kiely, G., Lewis, C., 2009. Estimation and analysis of soil hydraulic properties through infiltration experiments: comparison of BEST and DL fitting methods. Soil Use Manage. 25, 354–361.

FIGURE CAPTIONS

Fig. 1 Example of volumetric soil water content data collected by a TDR station with probes inserted below a row. The represented survey was performed during the first irrigation event at farm 2 (in 2008). The vertical line indicates the end of the irrigation event. The 0.65 m depth data are missing because a layer of stones prevented the insertion of a TDR probe.

Fig. 2 Example of soil water content profiles measured with the TDR technique every 5 minutes during the first irrigation event performed at farm 1 in 2006. The lines represent the water content profiles computed every 5 minutes from the beginning of the irrigation event, $t0$, until the end of the irrigation event. The vertical axis, z, indicates the soil depth.

Fig. 3 Diagram of an infiltration profile in which the whole water volume is subdivided into five portions. The horizontal black line represents the field surface, and the vertical line represents the end of the field. The data represent the real irrigation event performed on July 2008 at farm 3.

Fig. 4 Comparison of the saturated hydraulic conductivity values estimated by seven different well-known pedotransfer functions and the field-equivalent values estimated by the proposed method (Ks_eq). The tested pedotransfer functions are indicated as follows: Cosby et al. (1984) = (Ks_C); Saxton et al. (1986) = (Ks_S); Brakensiek et al. (1984) = (Ks_B); Ferrer-Julià et al. (2004) = (Ks_F); Campbell and Shiozawa (1994) = (Ks_CS); Puckett et al. (1985) = (Ks_P); and Dane and Puckett (1994)= (Ks_DP).

Fig. 5 Soil water infiltration profiles observed during the first irrigation event performed at farm 1 in 2007. The circles represent the depths of water infiltration that were measured using TDR probes. The curved lines represent the water content profiles calculated every 5 minutes from the beginning of the irrigation event ($t0$) until the end of the irrigation event (t_{ir}). The imposed hydraulic head (dash-dotted line) corresponds to the volume of water stored on the field surface divided by the total surface. The vertical axis, z, indicates the soil depth.

Fig. 6 Application efficiencies (E_a) (a), storage efficiencies (E_s) (b) and distribution efficiencies (E_d) (c) calculated from the infiltration profiles obtained by using the field-equivalent saturated hydraulic conductivity values and the three sets of saturated hydraulic conductivity values estimated by the BEST infiltration tests. The irrigation events (x axis) are identified as farm: irrigation event: year.

Fig. 7 Infiltration-profile scenario analysis based on the data collected during the first irrigation event performed at farm 1 in 2007. The real case is depicted in box (a) whilst the simulated cases, obtained by modifying the soil and irrigation parameters, are shown in boxes (b to h). The values of the parameters for the scenarios are listed in each single box: initial soil water content (θ_i), watering volume (V_d), flow rate (F_r) and irrigation duration (t_{ir}).

(a) The circles represent the depths of water infiltration measured using the TDR technique. The dotted vertical line and dashed vertical line indicate the locations of the two TDR probe profiles, which were located at 30 m and 32 m from the beginning of the field, respectively.

TABLE CAPTIONS

Tab. 1 Saturated and field-capacity water content values of the examined soils.

Tab. 2 Soil texture and the percentages of stones in the three different farm soils monitored.

Tab. 3 Plot size variability during the three-year monitoring period.

Tab. 4 Relationship between the water volume stored on the surface (V_s) and the water volume stored in the root layer (V_{rt}) for the fifteen monitored irrigation events.

Tab. 5 Calculated values of the dimensionless parameters t_k (-), C_k (-), and x_k (-) for the Philip and Farrell analytical solution.

Tab. 6 Field-equivalent saturated hydraulic conductivity values (cm h^{-1}) calculated for each farm and each year during the period from 2006-2008.

Tab. 7 Saturated hydraulic conductivity values (cm h^{-1}) estimated by means of the three BEST tests for each farm and each year during the period from 2006-2008. Differences between estimated saturated hydraulic conductivity and corresponding K_{Seq} values are given in brackets as percentage of saturated hydraulic conductivity.

Tab. 8 RMSE calculated between the K_{Seq} values and the K_S values estimated by pedotransfer functions and BEST tests.

Tab. 9 Differences between simulated and measured infiltration depths. The differences were calculated at 180 s (t_1), 360 s (t_2), 540 s (t_3), 720 s (t_4) from the start of the irrigation events and at the end of them (t_{ir}) at the locations of the TDR profiles (30 m - x_1 - and 32 m - x_2 - from the beginning of the field).

Tab. 10 Volumetric soil water content at the beginning of the irrigation event (θ_i), irrigation water volume (V_d), flow rate (F_r), irrigation event duration (t_{ir}), time required for the water front to reach the end of the field (t_f), field length (F_l), and values of the water application efficiency (E_a), water storage efficiency (E_s), and water distribution efficiency (E_d) for each irrigation event monitored during the period from 2006-2008.

Tab. 11 Volumetric soil water content at the beginning of each irrigation event (θ_i), irrigation water volume (V_d), flow rate (F_r), irrigation event duration (t_{ir}), field length (F_l), and values of the water application efficiency (E_a), water storage efficiency (E_s), and water distribution efficiency (E_d) for the first irrigation event performed at farm 1 in 2007 and the seven simulated scenarios.

TABLES

	Saturated soil water content ($m^3\ m^{-3}$)				Field capacity soil water content ($m^3\ m^{-3}$)			
	2006	**2007**	**2008**	**Average**	**2006**	**2007**	**2008**	**Average**
Farm 1	0.405	0.398	0.424	0.409	0.347	0.341	0.363	0.350
Farm 2	0.454	0.419	0.440	0.438	0.391	0.361	0.379	0.377
Farm 3	0.426	0.414	0.427	0.422	0.381	0.371	0.382	0.378

Table 1

Farm	Sand (%)	Silt (%)	Clay (%)	Stones (%)	Texture
1	20.4	71.1	8.5	20	Silty Loam
2	42.1	48.8	9.1	30	Loam
3	46.8	42.2	11	25	Loam

Table 2

	2006		2007		2008	
Farm	**Length (m)**	**Width (m)**	**Length (m)**	**Width (m)**	**Length (m)**	**Width (m)**
1	130	35	88	35	88	35
2	134	120	134	120	229	11
3	600	96	600	96	600	96

Table 3

	Irrigation event - year	V_s/V_{rt} ($m^3\ m^{-3}$)
Farm 1	1 - 2006	0.10
	4 - 2006	0.04
	1 - 2007	0.06
	2 - 2007	0.09
	1 - 2008	0.09
Farm 2	2 - 2006	0.10
	3 - 2006	0.10
	1 - 2007	0.10
	1 - 2008	0.03
Farm 3	2 - 2006	0.04
	4 - 2006	0.05
	1 - 2007	0.05
	2 - 2007	0.10
	1 - 2008	0.08
	4 - 2008	0.10

Table 4

	Farm 1					Farm 2				Farm 3					
	2006		2007		2008	2006		2007	2008	2006		2007		2008	
	1	4	1	2	1	2	3	1	1	2	4	1	2	1	4
τ_k	0.01	0.01	0.01	0.01	0.01	0.02	0.01	0.02	0.02	0.03	0.03	0.03	0.03	0.04	0.04
C_k	0.21	0.11	0.07	0.07	0.19	0.1	0.15	0.14	0.13	0.11	0.13	0.12	0.16	0.15	0.18
x_k	0.05	0.10	0.10	0.09	0.07	0.19	0.10	0.13	0.12	0.23	0.22	0.26	0.18	0.23	0.22

Table 5

	2006	2007	2008	Average	Standard deviation
Farm 1	2.47	2.38	2.51	2.45	0.12
Farm 2	4.64	5.02	1.76	3.81	1.17
Farm 3	2.28	2.52	2.85	2.55	0.30

Table 6

	BEST test 1			BEST test 2			BEST test 3		
	2006	**2007**	**2008**	**2006**	**2007**	**2008**	**2006**	**2007**	**2008**
Farm 1	2.34	2.31	2.25	2.41	2.44	2.48	2.63	2.52	2.57
	(5.3%)	(2.9%)	(10.4%)	(2.4%)	(-2.5%)	(1.2%)	(-6.5%)	(-7.1%)	(-2.4%)
Farm 2	3.96	3.18	1.61	4.35	4.28	1.87	4.66	4.91	2.48
	(14.7%)	(36.7%)	(8.5%)	(6.3%)	(14.7%)	(-6.3%)	(-0.4%)	(-40.9%)	(2.2%)
Farm 3	1.93	2.36	2.51	2.16	2.48	2.73	2.54	2.51	3.07
	(15.7%)	(7.8%)	(12.2%)	(5.7%)	(3.1%)	(4.5%)	(-10.9%)	(2.0%)	(-7.3%)

Table 7

	Ks_C	Ks_S	Ks_B	Ks_F	Ks_CS	Ks_P	Ks_DP	Ks_BEST #1	Ks_BEST #2	Ks_BEST #3
RMSE	1.54	2.73	3.06	2.49	3.00	0.62	6.10	0.69	0.28	0.28

Table 8

		t_1	t_2	t_3	t_4	t_{ir}
Farm 1 x_1	1 - 2006	0.012	0.009	0.005	-0.005	-0.012
	4 - 2006	0.006	0.007	0.006	0.003	-0.002
	1 - 2007	0.003	0.005	-0.009	-0.013	-0.013
	2 - 2007	0.006	-0.003	0.004	-0.004	-0.005
	1 - 2008	0.007	0.005	0.004	-0.007	-0.006
Farm 1 x_2	1 - 2006	0.008	0.006	0.007	-0.003	-0.093
	4 - 2006	0.003	0.008	0.007	0.004	-0.007
	1 - 2007	0.006	0.002	0.002	-0.005	-0.004
	2 - 2007	0.007	0.004	0.005	-0.004	0.003
	1 - 2008	0.011	0.01	0.012	0.009	0.004
Farm 2 x_1	2 - 2006	0.007	0.004	-0.005	0.006	0.01
	3 - 2006	0.006	0.006	0.007	-0.004	-0.018
	1 - 2007	0.011	0.018	0.004	-0.006	-0.004
	1 - 2008	0.01	0.007	0.005	-0.008	-0.005
Farm 2 x_2	2 - 2006	0.006	-0.003	-0.008	-0.009	-0.012
	3 - 2006	0.004	0.004	0.002	-0.003	-0.007
	1 - 2007	0.018	0.011	0.006	-0.003	-0.008
	1 - 2008	0.007	0.013	0.01	0.005	0.005
Farm 3 x_1	1 - 2006	0.003	0.003	0.005	-0.006	-0.008
	4 - 2006	0.009	0.008	0.01	-0.004	-0.005
	1 - 2007	0.004	0.007	0.011	0.008	-0.006
	2 - 2007	0.011	0.012	0.015	0.003	-0.01
	1 - 2008	-0.017	-0.018	-0.005	-0.003	0.012
	4 - 2008	-0.008	-0.007	-0.005	-0.011	0.007
Farm 3 x_2	1 - 2006	0.011	0.009	0.006	0.004	-0.009
	4 - 2006	0.007	0.012	0.008	-0.005	-0.004
	1 - 2007	-0.006	0.004	0.012	0.009	-0.009
	2 - 2007	0.012	0.011	0.009	0.004	-0.006
	1 - 2008	-0.01	-0.01	-0.006	-0.003	0.011
	4 - 2008	-0.007	-0.006	-0.003	-0.008	0.009

Table 9

	Monitored irrigation event - year	θ_i ($m^3\ m^{-3}$)	V_d ($m^3\ ha^{-1}$)	F_r ($m^3\ s^{-1}$)	t_{ir} (*s*)	t_{fl} (*s*)	F_l (m)	E_a (-)	E_s (-)	E_d (-)
Farm 1	1 - 2006	0.08	838	0.054	1513	1505	130	1.00	0.67	0.47
	4 - 2006	0.12	741	0.048	1505	1505	130	1.00	0.63	0.46
	1 - 2007	0.12	706	0.051	913	594	88	0.92	0.81	0.70
	2 - 2007	0.08	706	0.051	913	675	88	0.95	0.59	0.64
	1 - 2008	0.14	1482	0.060	1630	467	88	0.67	0.87	0.89
Farm 2	2 - 2006	0.05	1772	0.125	1797	1034	130	0.72	0.99	0.97
	3 - 2006	0.13	1183	0.125	1200	843	130	0.81	0.96	0.86
	1 - 2007	0.12	1119	0.125	1135	898	130	0.72	0.98	0.92
	1 - 2008	0.13	1817	0.160	2925	784	229	0.53	1.00	1.00
Farm 3	2 - 2006	0.12	1352	0.123	3957	3825	600	0.79	0.93	0.72
	4 - 2006	0.16	1409	0.128	3963	3144	600	0.69	0.98	0.93
	1 - 2007	0.08	1829	0.138	4771	3727	600	0.69	0.98	0.94
	2 - 2007	0.13	1577	0.159	3571	2326	600	0.65	1.00	0.99
	1 - 2008	0.07	2249	0.156	5190	3543	600	0.59	1.00	1.00
	4 - 2008	0.18	1791	0.161	4005	2250	600	0.60	1.00	1.00

Table 10

	Irrigation event - year	θ_i ($m^3\ m^{-3}$)	V_d ($m^3\ ha^{-1}$)	F_r ($m^3\ s^{-1}$)	*t* (*s*)	F_l (m)	E_a (-)	E_s (-)	E_d (-)
Farm 1	2 - 2007 - real case	0.12	706	0.051	913	88	0.92	0.81	0.70
	2 - 2007 - case 1	0.12	727	0.040	1200	88	0.95	0.87	0.64
	2 - 2007 - case 2	0.12	970	0.040	1600	88	0.79	0.97	0.89
	2 - 2007 - case 3	0.12	1236	0.051	1600	88	0.64	1.00	1.00
	2 - 2007 - case 4	0.12	830	0.060	913	88	0.80	0.84	0.82
	2 - 2007 - case 5	0.12	968	0.070	913	88	0.71	0.86	0.89
	2 - 2007 - case 6	0.05	706	0.051	913	88	0.97	0.70	0.61
	2 - 2007 - case 7	0.15	706	0.051	913	88	0.86	0.92	0.79

Table 11

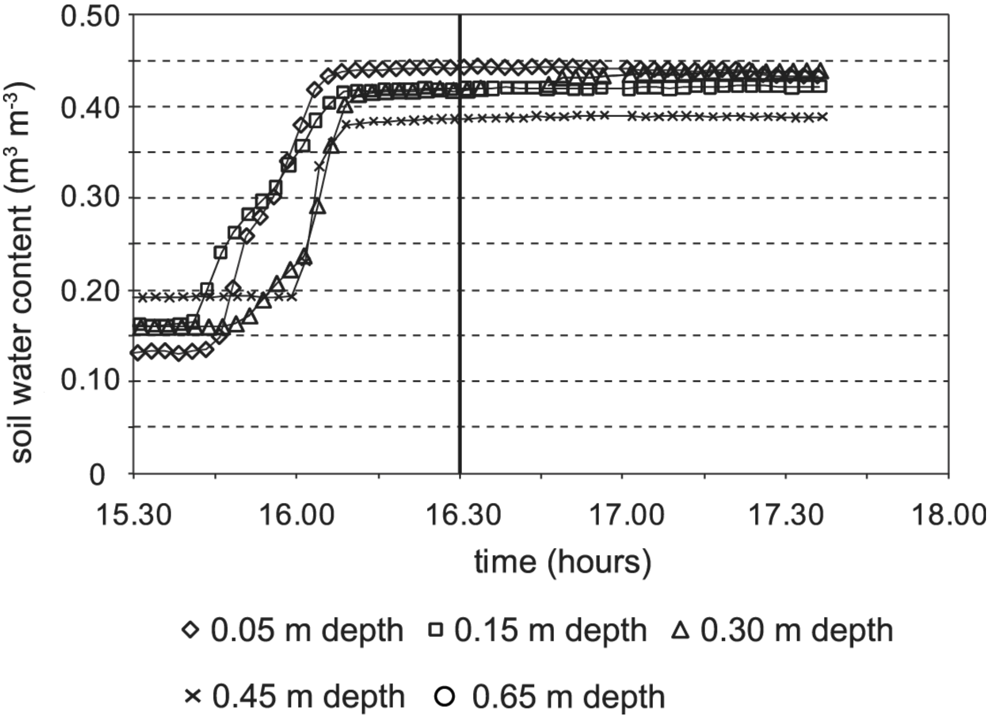

Figure 1

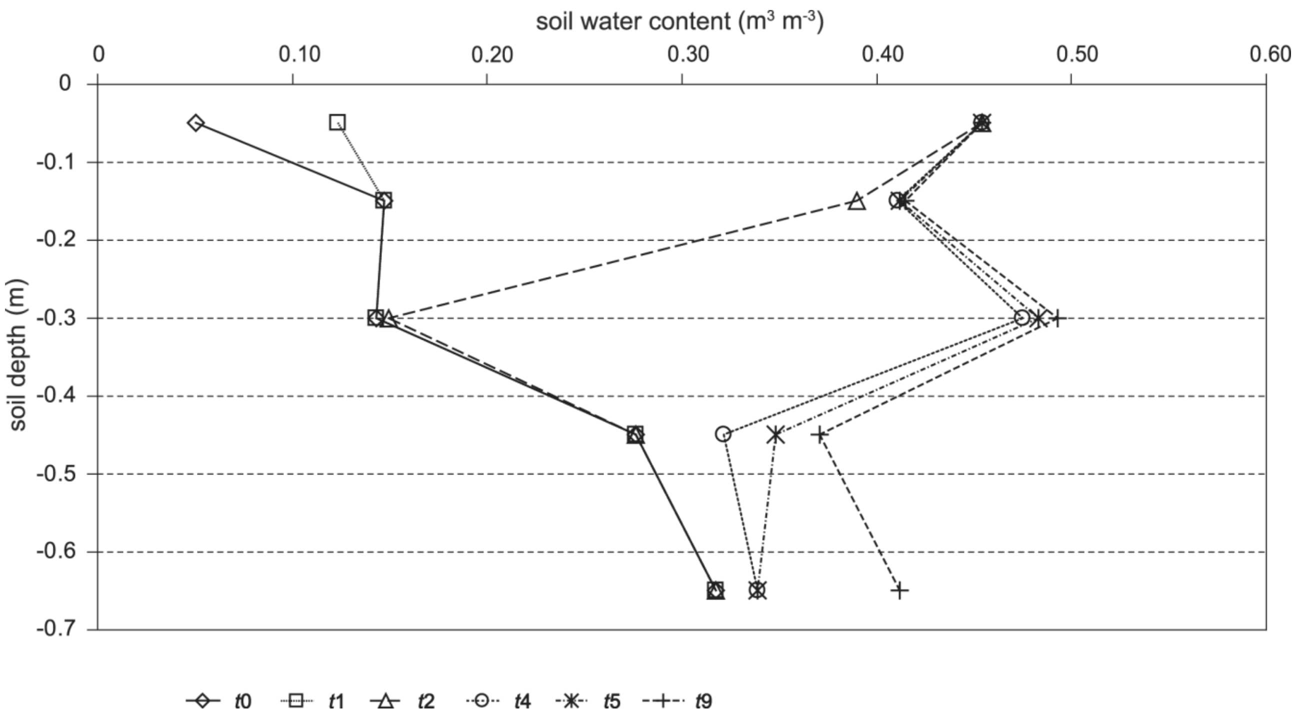

Figure 2

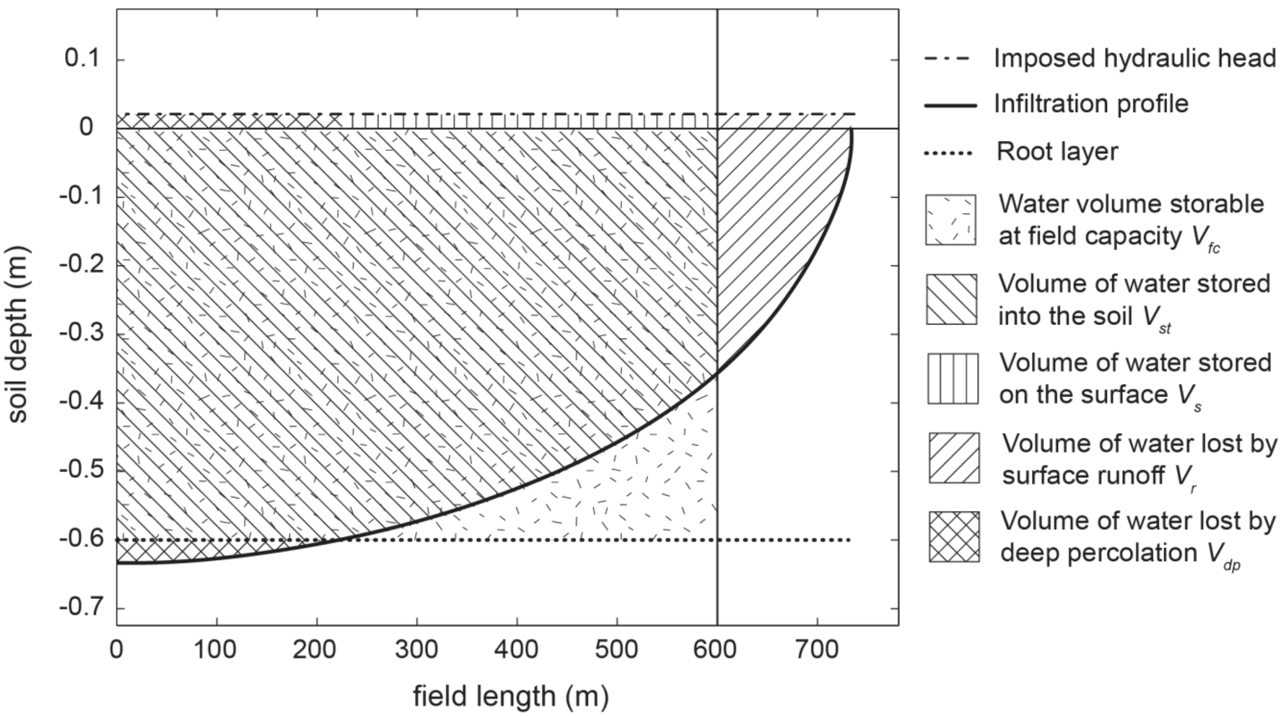

Imposed hydraulic head
Infiltration profile
Root layer
Water volume storable at field capacity V_{fc}
Volume of water stored into the soil V_{st}
Volume of water stored on the surface V_s
Volume of water lost by surface runoff V_r
Volume of water lost by deep percolation V_{dp}
soil depth (m)
field length (m)
0.1
0
-0.1
-0.2
-0.3
-0.4
-0.5
-0.6
-0.7
0
100
200
300
400
500
600
700

Figure 3

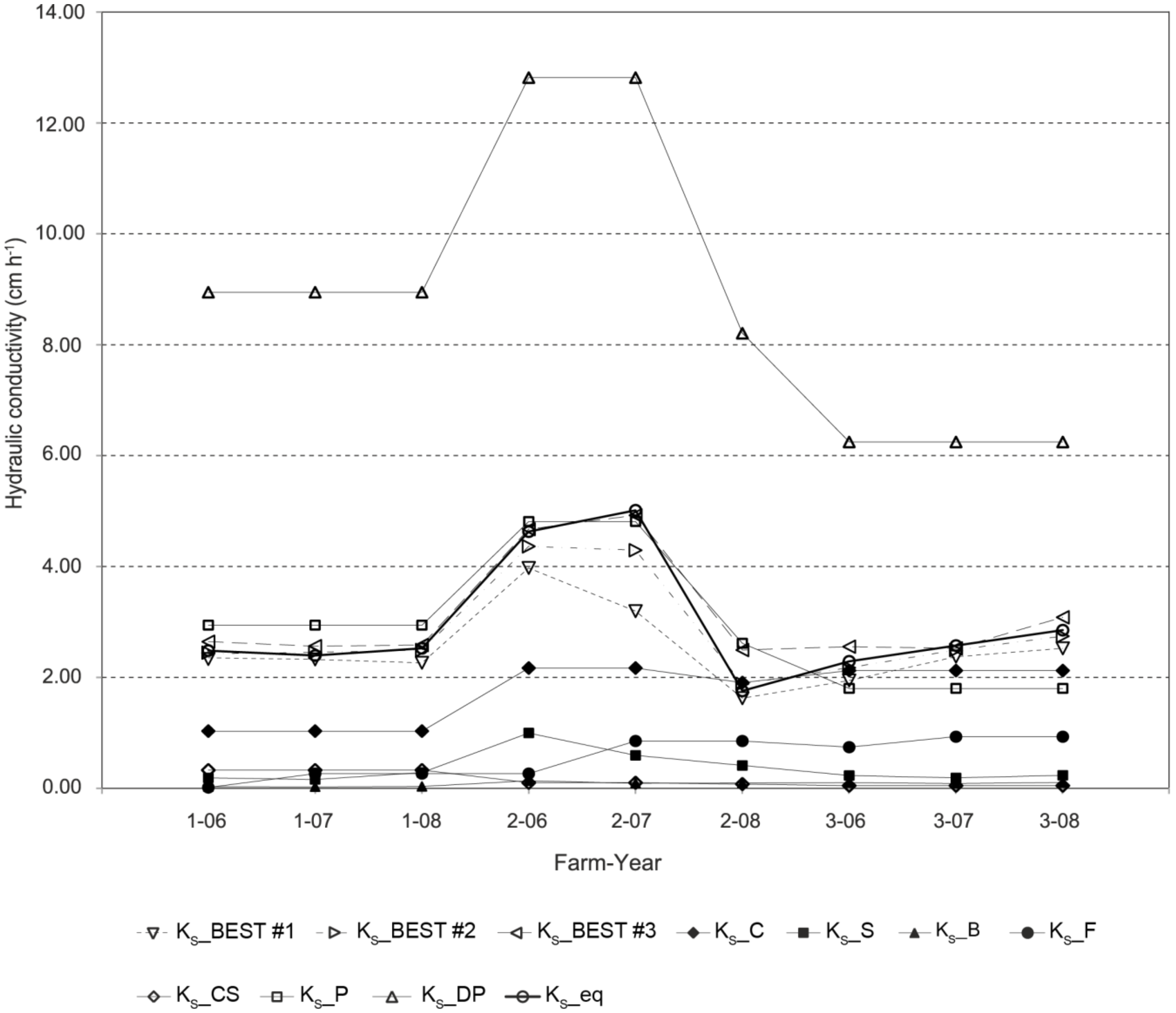

14.00
12.00
10.00
8.00
6.00
4.00
2.00
0.00
Hydraulic conductivity (cm h-1)
1-06
1-07
1-08
2-06
2-07
2-08
3-06
3-07
3-08
Farm-Year
KS_BEST #1
KS_BEST #2
KS_BEST #3
KS_C
KS_S
KS_B
KS_F
KS_CS
KS_P
KS_DP
KS_eq

Figure 4

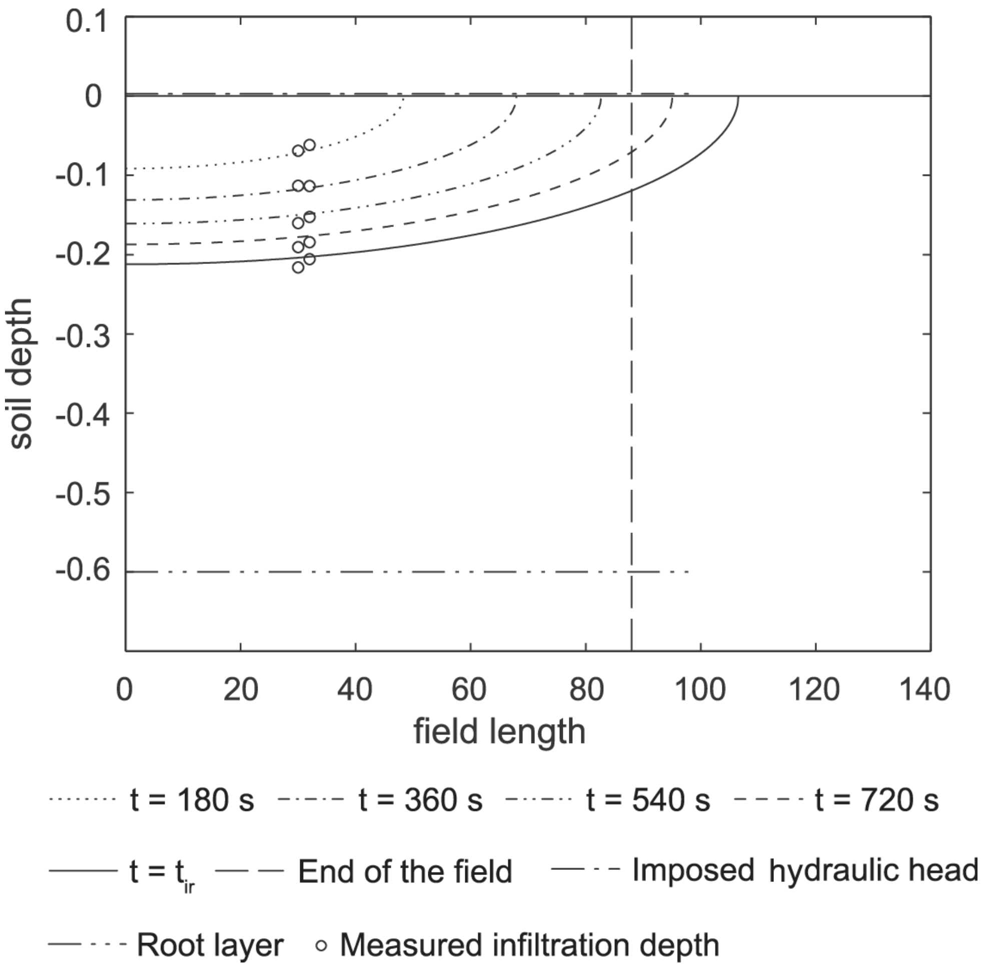
0.1
0
-0.1
-0.2
-0.3
-0.4
-0.5
-0.6
soil depth
0
20
40
60
80
100
120
140
field length
t = 180 s
t = 360 s
t = 540 s
t = 720 s
t = t_ir
End of the field
Imposed hydraulic head
Root layer
Measured infiltration depth

Figure 5

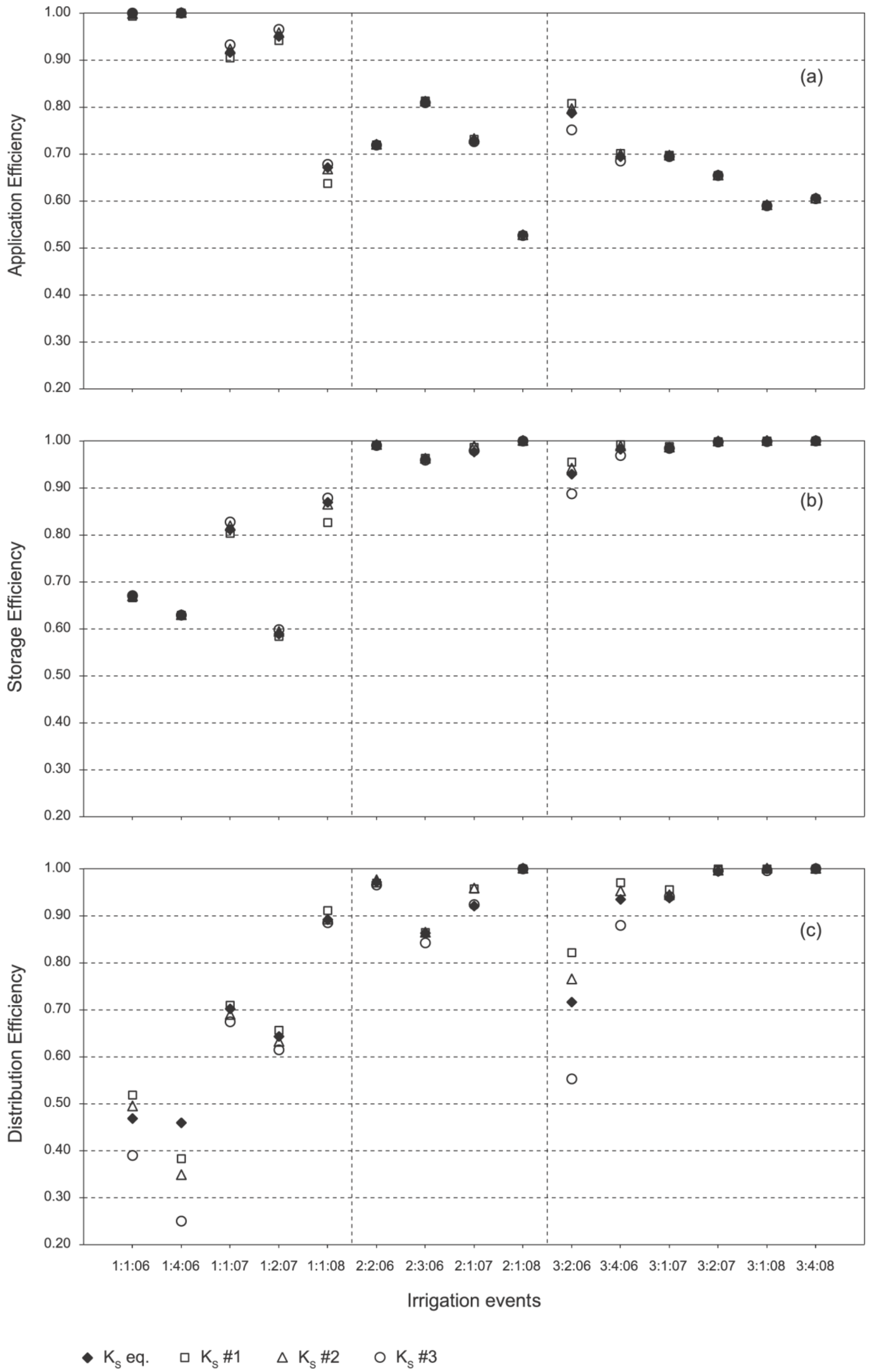
Application Efficiency
(a)
Storage Efficiency
(b)
Distribution Efficiency
(c)
1.00
0.90
0.80
0.70
0.60
0.50
0.40
0.30
0.20
1:1:06 1:4:06 1:1:07 1:2:07 1:1:08 2:2:06 2:3:06 2:1:07 2:1:08 3:2:06 3:4:06 3:1:07 3:2:07 3:1:08 3:4:08
Irrigation events
K_s eq. K_s #1 K_s #2 K_s #3

Figure 6

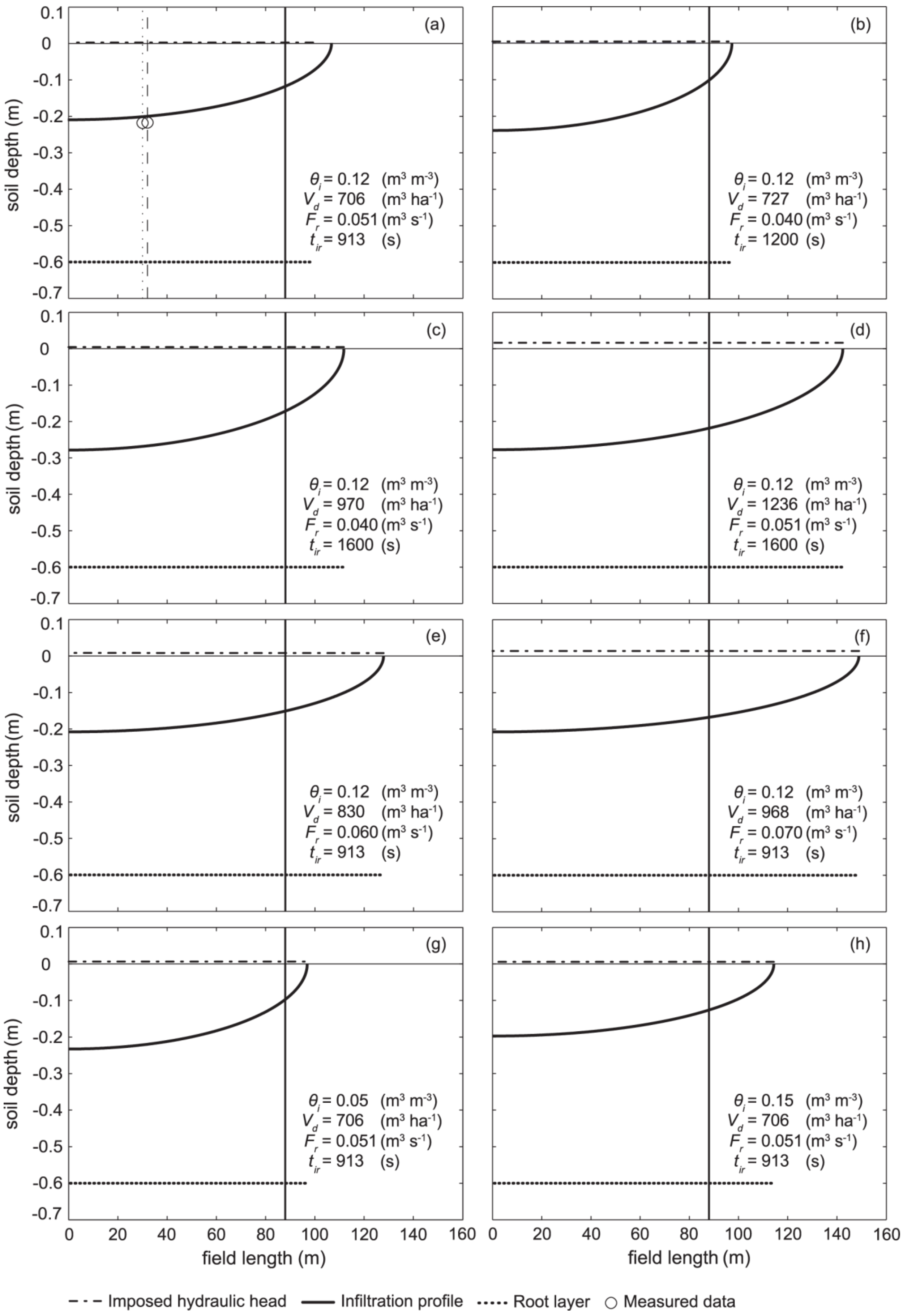

(a)
(b)
(c)
(d)
(e)
(f)
(g)
(h)
soil depth (m)
field length (m)
θi = 0.12 (m³ m⁻³)
Vd = 706 (m³ ha⁻¹)
Fr = 0.051 (m³ s⁻¹)
tir = 913 (s)
θi = 0.12 (m³ m⁻³)
Vd = 727 (m³ ha⁻¹)
Fr = 0.040 (m³ s⁻¹)
tir = 1200 (s)
θi = 0.12 (m³ m⁻³)
Vd = 970 (m³ ha⁻¹)
Fr = 0.040 (m³ s⁻¹)
tir = 1600 (s)
θi = 0.12 (m³ m⁻³)
Vd = 1236 (m³ ha⁻¹)
Fr = 0.051 (m³ s⁻¹)
tir = 1600 (s)
θi = 0.12 (m³ m⁻³)
Vd = 830 (m³ ha⁻¹)
Fr = 0.060 (m³ s⁻¹)
tir = 913 (s)
θi = 0.12 (m³ m⁻³)
Vd = 968 (m³ ha⁻¹)
Fr = 0.070 (m³ s⁻¹)
tir = 913 (s)
θi = 0.05 (m³ m⁻³)
Vd = 706 (m³ ha⁻¹)
Fr = 0.051 (m³ s⁻¹)
tir = 913 (s)
θi = 0.15 (m³ m⁻³)
Vd = 706 (m³ ha⁻¹)
Fr = 0.051 (m³ s⁻¹)
tir = 913 (s)
Imposed hydraulic head
Infiltration profile
Root layer
Measured data

Figure 7